Published in final edited form as:

Mol Cancer Res. 2015 December ; 13(12): 1533–1543. doi:10.1158/1541-7786.MCR-15-0237.

Hypoxia Promotes Synergy between Mitomycin C and Bortezomib through a Coordinated Process of Bcl-xL Phosphorylation and Mitochondrial Translocation of p53

Xinxin Song[1], **Ashok-Kumar Dilly**[1], **Haroon Asif Choudry**[1], **David L. Bartlett**[1], **Yong Tae Kwon**[3], and **Yong J. Lee**[1,2,*]

[1]Department of Surgery, University of Pittsburgh Cancer Institute, School of Medicine, University of Pittsburgh, Pittsburgh, Pennsylvania 15213, USA

[2]Department of Pharmacology & Chemical Biology, University of Pittsburgh Cancer Institute, School of Medicine, University of Pittsburgh, Pittsburgh, Pennsylvania 15213, USA

[3]Protein Metabolism Medical Research Center and Department of Biomedical Science, College of Medicine, Seoul National University, Seoul 110-799, Korea

Abstract

Colorectal peritoneal carcinomatosis (CPC) exhibits severe tumor hypoxia, leading to drug resistance and disease aggressiveness. This study demonstrates that the combination of the chemotherapeutic agent mitomycin C with the proteasome inhibitor bortezomib induced synergistic cytotoxicity and apoptosis, which was even more effective under hypoxia in colorectal cancer cells. The combination of mitomycin C and bortezomib at sub-lethal doses induced activation of c-Jun NH2-terminal kinase and p38 mitogen-activated protein kinase and resulted in Bcl-xL phosphorylation at Serine 62, leading to dissociation of Bcl-xL from pro-apoptotic Bak. Interestingly, the intracellular level of p53 became elevated and p53 translocated to the mitochondria during the combinatorial treatment, in particular under hypoxia. The coordinated action of Bcl-xL phosphorylation and p53 translocation to the mitochondria resulted in conformational activation of Bak oligomerization, facilitating cytochrome *c* release and apoptosis induction. In addition, the combinatorial treatment with mitomycin C and bortezomib significantly inhibited intraperitoneal tumor growth in LS174T cells and increased apoptosis, especially under hypoxic conditions *in vivo*. This study provides a preclinical rationale for the use of combination therapies for CPC patients.

All correspondence should be addressed to Dr. Yong J. Lee, Department of Surgery, University of Pittsburgh, Hillman Cancer Center, 5117 Centre Ave. Room 1.46C, Pittsburgh, PA 15213, U.S.A., Tel (412) 623-3268, Fax (412) 623-7709, leeyj@upmc.edu.

Conflict-of-interest disclosure: The authors declare no competing financial interests.

Disclosure of Potential Conflicts of Interest
No potential conflicts of interest were disclosed.

Authors' Contributions
Conception and design: Y.J. Lee, D.L. Bartlett
Development of methodology: X. Song, Y.T. Kwon
Acquisition of data: X. Song, A.-K. Dilly, H.A. Choudry
Analysis and interpretation of data: X. Song, Y.J. Lee
Writing, Review, and/or revision of the manuscript: X. Song, Y.J. Lee
Administrative, technical, or material support: Y.J. Lee, D.L. Bartlett, Y.T. Kwon
Study supervision: Y.J. Lee

Implications—The combination of a chemotherapy agent and proteasome inhibitor at sub-lethal doses induced synergistic apoptosis, in particular under hypoxia, *in vitro* and *in vivo* through coordinated action of Bcl-xL and p53 on Bak activation.

Keywords

Mitomycin C; Botezomib; Hypoxia; Apoptosis; p53; Bcl-xL

Introduction

Peritoneal carcinomatosis (PC) is regarded as the most common lethal primary or secondary cancerous disease that affects the peritoneal cavity following colorectal cancer, appendiceal cancer, ovarian cancer, gastric cancer, or diffuse malignant peritoneal mesothelioma (1, 2). Colorectal peritoneal carcinomatosis (CPC), which affects approximately 10% of colorectal cancer patients, is one manifestation of metastatic colorectal cancer (2, 3). Standard treatments involve cytoreductive surgery and perioperative chemotherapy (4). However, CPC is generally considered an untreatable condition that makes clinicians abandon further aggressive treatment, and the response rates of CPC patients are low (4). Physiologic stress from hypoxia, a feature of most tumors, has been associated with the resistance of CPC to therapy (5).

Bioreductive prodrugs have been designed to be activated under hypoxia and thus increase achievable therapeutic effects under hypoxic conditions. Some agents have also been developed to target hypoxic tumor cells through inhibition of hypoxia-inducible factor (HIF) 1, a master transcriptional regulator (6). The chemotherapeutic agent mitomycin C is a naturally occurring, clinically used, bioreductive alkylating prodrug that is activated by several enzymes, including cytochrome P450 reductase (7). Mitomycin C has also been shown to inhibit HIF-1α protein synthesis (8). It has been tested in a great number of preclinical and clinical studies and is widely used to treat PC (9). However, mitomycin C alone is not potent enough to generate sustained tumor regression and has been shown cause unexpected side effects (10, 11). Therefore, we should consider combinations of cytotoxic drugs and other agents that have achieved improvement in animal models and patients (12–14), thereby enhancing the likelihood of survival for CPC patients.

The ubiquitin-proteasome pathway has been well recognized as a valid target for anti-tumor therapy and is also regarded as a biomarker of poor prognosis for peritoneal mesothelioma tumors (15). Bortezomib, an approved-for-clinical-use proteasome inhibitor used to treat multiple myeloma, induces apoptosis in a wide variety of cancer cell lines, yet has relatively few toxic effects on normal cells (16–18). However, bortezomib has minimal activity as a single agent in the treatment of recurrent platinum-sensitive epithelial ovarian or primary peritoneal cancer, indicating that proteasome inhibitors should be combined with other reagents to increase the effectiveness of therapy (19, 20).

In this study, we observed that the combination of the chemotherapeutic agent mitomycin C and the proteasome inhibitor bortezomib in sub-lethal doses induced synergistic cytotoxicity and apoptosis, in particular under hypoxia *in vitro* and *in vivo*. The combination of mitomycin C and bortezomib induced oligomerization of Bcl-2 homologous antagonist/

killer (Bak) through coordinated action of Bcl-xL dissociation from Bak and p53 mitochondrial localization and resulted in mitochondria-dependent apoptotic cell death. The significance of our findings promotes the opportunity to incorporate bortezomib with mitomycin C to preferentially target not only normoxic, but also hypoxic tumor cells, allowing for more effective therapy for CPC patients.

Materials and Methods

Cell cultures and transfection

Human colorectal carcinoma CX-1 cells, which were obtained from Dr. J.M. Jessup (Division of Cancer Treatment and Diagnosis, National Cancer Institute, National Institutes of Health), were cultured in RPMI-1640 medium containing 10% fetal bovine serum (FBS). Human colorectal carcinoma HCT116 cells, kindly provided by Dr. B. Vogelstein (Johns Hopkins University, Baltimore, MD, USA), were cultured in McCoy's 5A medium containing 10% FBS. LS174T and LS180 are human colon adenocarcinoma cell lines and were purchased from American Type Culture Collection (ATCC, Manassas, VA, USA) and cultured in Eagle's Minimum Essential Medium and 10% FBS at 37°C and 5% CO_2. Mycoplasma testing was conducted routinely for all cell lines. For transient transfection, cells were transfected with Lipofectamine 2000 (Life Technologies, Gaithersburg, MD, USA) and were treated 48 h after transfection.

Hypoxic treatment

Hypoxic cell culture experiments were carried out at 1% O_2 using a hypoxia chamber (Anaerobic System model 1025/1029, ThermoForma; Waltham, MA, USA).

Reagents and antibodies

Mitomycin C was obtained from Santa Cruz Biotechnology (Santa Cruz, CA, USA). Bortezomib was obtained from Millennium Pharmaceuticals (Cambridge, MA, USA). Anti-hemagglutinin (HA), anti-Bcl-xL, anti- carcinoembryonic antigen (CEA), anti-phospho-c-Jun NH2-terminal kinase (JNK), anti-JNK, anti-Bak, anti-caspase 8, anti-caspase 9, anti-caspase 3, anti-Bad, anti-p-p53(Ser46)/p53, anti-COX IV antibody, and anti-poly (ADP-ribose) polymerase (PARP) antibody came from Cell Signaling (Danvers, MA, USA). Anti-actin antibody came from Sigma-Aldrich (St. Louis, Missouri, USA). Anti-p-Bcl-xL (S62) antibody was obtained from Millipore (Bedford, MA, USA). Anti-cytochrome *c* antibody came from BD PharMingen (San Jose, CA, USA). Anti-Ki67 antibody was purchased from Dako (Carpinteria, CA, USA).

MTS [3-(4,5-dimethylthiazol-2-yl)-5-(3-carboxymethoxyphenyl)-2-(4-sulfophenyl)-2H-tetrazolium] assays

MTS studies were carried out using the Promega CellTiter 96 AQueous One Solution Cell Proliferation Assay (Promega, Madison, WI, USA). Cells were then treated with MTS/phenazine methosulfate solution for 1 h at 37°C. Absorbance at 490 nm was determined using an enzyme-linked immunosorbent assay plate reader.

Annexin V binding

Cells were harvested with trypsinization, washed with serum-free medium, and suspended in binding buffer (annexin V-fluorescein isothiocyanate (FITC) Staining Kit, BD PharMingen). This cell suspension was stained with FITC-conjugated annexin V and propidium iodide (PI) and then immediately analyzed using flow cytometry.

Combination index (CI) analysis

CIs were calculated using the CompuSyn software (ComboSyn, Inc., Paramus, NJ, USA). Base on CI values, the extent of synergism/antagonism was determined. In general, CI values below 1 suggest synergy, whereas CI values above 1 indicate antagonism between the drugs. CI values in the 0.9–1.10 range mainly indicate additive effects, those between 0.9–0.85 suggest slight synergy, those in the range of 0.7–0.3 indicate moderate synergy, and those less than 0.3 suggest strong synergy.

Immunoblot analysis

Cells were lysed with Laemmli lysis buffer and boiled for 10 min. Protein content was measured with BCA Protein Assay Reagent (Thermo Scientific, Hudson, NH, USA), separated by sodium dodecyl sulfate polyacrylamide gel electrophoresis (SDS-PAGE), and electrophoretically transferred to nitrocellulose membrane. The nitrocellulose membrane was blocked with 5% nonfat dry milk in phosphate buffered saline (PBS)-Tween-20 (0.1%, v/v) for 1 h and incubated with primary antibody at room temperature for 2 h. Horseradish peroxidase conjugated anti-rabbit or anti-mouse IgG was used as the secondary antibody. Immunoreactive protein was visualized using the chemiluminescence protocol. Gel densitometry was analyzed using the software Gel-pro application from Media Cybernetics (Rockville, MD, USA).

Immunoprecipitation

Briefly, cells were lysed in CHAPS lysis buffer with protease inhibitor cocktail (Calbiochem, San Diego, CA, USA). 0.5–1 mg of lysate was incubated with 1.5 μg of anti-Bak/HA antibody or rabbit IgG (Santa Cruz) at 4°C overnight, followed by the addition of protein G PLUS-agarose beads (Santa Cruz) and rotation at room temperature for 2 h followed by immunoblot analysis.

Bak oligomerization

Cells were pelleted and resuspended in Hoechst buffer. The cell suspension was homogenized, and spun at 1,000 × g for 15 min at 4°C. The supernatant was transferred and spun at 10,000 × g for 15 min at 4°C to pellet mitochondria. Aliquots of isolated mitochondrial fractions and cytosolic fractions were cross-linked with 1 mM dithiobis (Pierce, Rockford, IL, USA). Samples were subjected to SDS-PAGE under non-denaturing conditions followed by immunoblotting for Bak.

Confocal microscopy

Cells were stained with 300 nM MitoTracker (Life Technologies). Cells were washed three times with 0.5% bovine serum albumin in PBS, followed by fixation in 4%

paraformaldehyde for 15 min. Bak was stained with anti-Bak antibody. Nuclei were stained with 4′,6-diamidino-2-phenylindole (DAPI) (Cell Signaling). Slides were mounted and visualized in 0.4-μm sections using an OlympusFluoview 1000 confocal microscope and the companion software FV10-ASW2.1 under a 63X oil immersion objective.

Measurement of cytochrome c release

To determine the release of cytochrome *c* from the mitochondria, mitochondrial and cytosolic fractions were prepared using the Mitochondrial Fractionation Kit (Active Motif, Carlsbad, CA, USA) following company instructions and reagents included in the kit. Cytosolic fractions were subjected to SDS-PAGE and analyzed with immunoblotting using anti-cytochrome *c* antibody.

Knockdown of p53 with siRNA oligomers

Cells were transfected with 50 nM of p53 siRNA and control siRNA from Sigma Aldrich, using Lipofectamine 2000. Target sequences for preparing siRNAs of human p53 were as follows: 5′-GAC UCC AGU GGU AAU CUA C-3′ (sense strand) and 5′-GUA GAU UAC CAC UGG AGU C-3′ (complement strand). Expression levels were determined by immunoblot analysis.

Animal model

Nude mice (six weeks old, Taconic, Germantown, NY, USA) were intraperitoneally (i.p.) challenged with 5×10^5 LS174T cells expressing firefly luciferase, which was stably transduced by lentiviral transfection of the pGL4 Luciferase Reporter Vector (Promega, Madison, WI, USA) and selected with puromycin. The luciferase signal was monitored by injecting the luciferase substrate luciferin (150 mg/kg, i.p.; GoldBio, St Louis, MO, USA) 5 min after anesthesia with 2% isoflurane prior to imaging on an IVIS200 system (Perkin Elmer, Waltham, MA, USA). Bioluminescence signal was quantified using the LivingImage software (Perkin Elmer). The mice were examined for bioluminescent signals, indicating basal tumor loading. Mice with the same bioluminescence levels were divided into four groups (five per group) and subjected to different treatments, including control, bortezomib (0.5mg/kg, i.p.) alone, mitomycin C (1.5 mg/kg, i.p.) alone, or bortezomib and mitomycin C in combination. Each group of mice was treated every other day. The tumor load, represented by bioluminescent signal determined using the IVIS bioluminescent Imaging System, was checked from week 1 to week 5. Mice were fed *ad libitum* and maintained in environments with controlled temperatures of 22–24°C and 12 h light and dark cycles. All animal experiments were carried out at the University of Pittsburgh in accordance with the Guide for the Care and Use of Laboratory Animals.

Immunohistochemical staining and immunofluorescent analysis

For immunohistochemical staining, tumor tissues recovered from each group were fixed in 10% neutral buffered formalin and embedded in paraffin. Sections were cut 4-μm thick and then were stained either via standard hematoxylin and eosin (H&E) staining or immunohistochemical staining with mAbs specific for human CEA and Ki67 and were

visualized with the Envision + dual link system (Dako) following the manufacturer's instructions.

Pimonidazole (60 mg/kg, Hypoxyprobe, Inc., Burlington, MA, USA) was administered 60 min i.p. prior to sacrifice of the mice. For quantification of hypoxic tumor cell apoptosis via immunofluorescence, tumors were fixed in 4% paraformaldehyde, 30% sucrose overnight, and then frozen in optimum cutting temperature (OCT) and cryosectioned. Sections were incubated with anti-cleaved caspase 3 antibody and mouse anti-pimonidazole Dylight™549-Mab, and then incubated with anti-Rabbit Alexa Fluor 488. The percentage of cleaved caspase 3 positive cells was quantified by counting at least 300 cells for each sample and plotted as mean ± S.D. of two independent experiments.

Pictures were taken using an Olympus BH2 microscope (Olympus, Tokyo, Japan) with a camera (Coolsnap3.3; Photometrics, Tucson, AZ, USA). Tissue sections of inoculation sites were examined under an Olympus BX71 microscope (Olympus, Lake Success, NY, USA) equipped with Hoffman objective lenses (×40 or 20; Diagnostic Instruments, Sterling Heights, MI, USA) connected to a SPOT One Digital Camera (Diagnostic Instruments). Images were then processed using Adobe Photoshop software (Adobe, San Jose, CA, USA).

Statistical analysis

Statistical analysis was carried out using GraphPad InStat 3 software (GraphPad Software, Inc., San Diego, CA, USA). Data showing comparisons between two groups were assessed using the Student's t test. Comparisons among more than two groups were done using ANOVA with the appropriate *post hoc* testing. Statistical significance is marked with asterisks (*, $p<0.05$ and ** or ##, $p<0.01$).

Results

The combination of mitomycin C and bortezomib induced synergistic cytotoxicity and apoptosis in normoxia and hypoxia

First, we investigated the effect of mitomycin C and bortezomib at different doses on human colorectal HCT116, CX-1, and LS174T cancer cells. We observed that the hallmark feature of apoptosis, PARP cleavage, significantly increased with the combination treatment of mitomycin C and bortezomib in a dose-dependent manner in all tested cell lines (Fig. 1A). We then tested the cytotoxicity of the combination of mitomycin C and bortezomib in LS174T cells under both normoxic (21% O_2) and hypoxic (1% O_2) conditions using MTS assay. As shown in Fig. 1B, mitomycin C induced 17.1 ± 2.1% cell death under normoxia. Interestingly, mitomycin C induced 29.1 ± 3.4% cell death under hypoxia ($p<0.05$). Bortezomib at 10 nM barely induced cell death under normoxia as well as hypoxia. Notably, bortezomib enhanced the effect of mitomycin C under both normoxia and hypoxia. To clarify whether the cytotoxicity of the combination of mitomycin C and bortezomib was associated with apoptosis, flow cytometry assay annexin/PI was performed. We observed that the combination of mitomycin C and bortezomib induced greater apoptotic cell death (annexin V^+ PI^- + annexin V^+ PI^+) than any single drug treatment under both normoxia and hypoxia (Fig. 1C). We also analyzed the synergistic effect of the combination of mitomycin

c and bortezomib under hypoxic conditions using combination index (CI) as shown in Table. 1. CI values were less than 0.7 or 0.3 for the indicated doses of each drug under hypoxia, indicating moderate synergy or strong synergy.

The combination of mitomycin C and bortezomib induced activation of caspases, Bcl-xL phosphorylation, and p53 elevation under normoxia as well as hypoxia

Next, we examined whether the combination of mitomycin C and bortezomib promoted the caspase pathways under normoxia and hypoxia in human colorectal LS174T and LS180 cancer cells. It is well known that the intracellular level of hypoxia-inducible factor-1α (HIF-1α) is elevated under hypoxia due to inhibition of degradation (21–23). Indeed, data from immunoblot analysis demonstrated an elevation of HIF-1α under hypoxia in LS174T cells (inset of Fig 2A). We also observed that 2 μg/ml mitomycin C or 10 nM bortezomib alone had no significant apoptotic effect under normoxia (main of Fig. 2A), but the combination of mitomycin C and bortezomib resulted in significant activation of caspase 8, 9, and 3, as well as PARP cleavage. Interestingly, mitomycin C alone under hypoxia induced activation of caspases and PARP cleavage, while the activation and cleavage from the combination of mitomycin C and bortezomib was greatly increased. Similar results were obtained in LS180 cells (Fig. 2C).

To confirm the differential effect of mitomycin C under normoxia and hypoxia, LS174T cells were treated with various doses of mitomycin C. As shown in Fig. 2B, the effect of mitomycin C was significantly increased under hypoxia compared to that under normoxia, especially in low doses.

We next investigated the apoptotic death-related mitogen-activated protein kinase (MAPK) signaling pathways during treatment with combination of mitomycin C and bortezomib under normoxia and hypoxia (Figs. 3A and 3B). We observed phosphorylation (activation) of JNK as well as p38 along with Bcl-xL phosphorylation during treatment with the combination of mitomycin C and bortezomib, especially under hypoxic conditions in LS174T and LS180 cells. We also observed p53 elevation with mitomycin C treatment regardless of oxygen tensions in LS174T and LS180 cells. It is reported that activated p38 can phosphorylate p53 at Ser46 and phosphorylated p53 (p-p53) localizes to the mitochondria (24–27). Thus, we examined p-p53 (Ser46) and observed an increase in the level of p-p53 during treatment with mitomycin C, in particular under hypoxia, in both LS174T and LS180 cells (Figs. 3A and 3B).

Role of MAPK in Bcl-xL phosphorylation during treatment with mitomycin C and bortezomib under normoxia and hypoxia

Several researchers have reported that MAPK plays a critical role in the death receptor-initiated extrinsic as well as the mitochondrial intrinsic apoptotic pathways (28, 29). Pretreatment of SB203580, a p38 inhibitor, or SP600125, a JNK inhibitor, attenuated the drug combination-induced PARP cleavage and decreased Bcl-xL phosphorylation in both normoxic and hypoxic culture systems (Fig. 4A). These results suggest that activation of p38 and JNK plays a role in the drug combination treatment-induced apoptosis through phosphorylation of Bcl-xL. Our previous studies demonstrated that stress-induced Bcl-xL

phosphorylation occurs on serine 62 (S62) residue (30). We next examined the role of Bcl-xL phosphorylation at S62 in the drug combination treatment-induced apoptosis. LS174T cells were transiently transfected with a sham plasmid, wild-type Bcl-xL (Bcl-xL WT-HA) or phospho-defective Bcl-xL (Bcl-xL S62A-HA) and then treated with mitomycin C and bortezomib under normoxia and hypoxia. We observed that Bcl-xL-S62A reduced the drug combination-induced PARP cleavage compared with Bcl-xL-WT (left panel and right panel in Fig. 4B). These data suggest Bcl-xL phosphorylation at S62 is essential for the synergistic effect of mitomycin C- and bortezomib-induced apoptosis.

To further study the role of Bcl-xL phosphorylation at S62 in the synergistic effect of mitomycin C- and bortezomib-induced apoptosis, we examined the interaction between Bak and Bcl-xL during treatment with mitomycin C and bortezomib. Bcl-xL-WT and Bcl-xL-S62A transient transfected cells were employed and immunoprecipitation assay was conducted. Figure 4C shows that Bcl-xL WT dissociated from Bak during combined treatment with mitomycin C and bortezomib under both normoxia and hypoxia, whereas Bcl-xL-S62A still maintained the interaction with Bak during combined treatment with mitomycin C and bortezomib under both normoxia and hypoxia. These results suggest that phosphorylation of Bcl-xL at S62 leads to apoptosis through dissociation of Bcl-xL from Bak.

Role of p53 in synergistic apoptotic effects of mitomycin C in combination with bortezomib under normoxia and hypoxia

We then further investigated the role of p53 in apoptotic death during treatment with mitomycin C and bortezomib under normoxia and hypoxia. As shown in Fig. 5A, we observed that p53 knockdown abrogated the combinatorial treatment-induced PARP cleavage under both normoxia and hypoxia, suggesting the pro-apoptotic function of p53. In Fig. 5B, we also observed that p53 translocated to the mitochondria during treatment with mitomycin C under normoxia, and this effect was enhanced under hypoxia probably due to p53 phosphorylation at Ser46 (Figs. 3A and 3B). There is no difference in terms of p53 translocation during bortezomib treatment under normoxia compared to that under hypoxia. Consistently, cellular cytochrome *c* release from the mitochondria to the cytosol increased in the combinatorial treatment under hypoxia compared to that under normoxia. Data from confocal immunofluorescence microscopy assay (Fig. 5C) confirmed p53 accumulation in the nucleus and mitochondria during mitomycin C alone and the combinatorial treatment, in particular under hypoxia.

Next, we investigated the role of mitochondrial translocated p53. As shown in Fig. 5D, in the LS174T cell line, p53 bound to Bak during the combinatorial treatment of mitomycin C and bortezomib. Binding affinity increased during treatment with mitomycin C alone or the combinatorial treatment under hypoxia. We also observed the dissociation of Bcl-xL from Bak during the bortezomib treatment as well as during the combinatorial treatment, especially under hypoxia, which was due to Bcl-xL phosphorylation. Similar results were obtained in the LS180 cell line. The dissociated (activated) pro-apoptotic members Bak or Bcl-2–associated X protein (Bax) are well known to form pores in the mitochondrial outer membrane, which allows cytochrome *c* to release into the cytoplasm and induce caspase

cascade (31). LS174T, a Bax-null cell line (32), is a good model to study the role of Bak. Consistently, we observed increased multimeric Bak oligomerization during the treatment with mitomycin C and bortezomib, especially under hypoxia (Fig. 5E). Confocal assay also shows Bak clustering localized in the mitochondria during the combinatorial treatment, especially under hypoxia (Fig. 5F).

Effect of mitomycin C and bortezomib on the growth of LS174T intraperitoneal tumors

Finally, *in vivo* studies were performed to examine the effect of the combinatorial treatment with mitomycin C and bortezomib on the growth of LS174T intraperitoneal tumors. Figures 6A and 6B show that administration with bortezomib every other day at doses of 0.5 mg/kg significantly decreased tumor growth compared with the control group ($p < 0.01$). Mitomycin C alone caused a statistically significant decrease of tumor growth ($P < 0.01$). In particular, the combinatorial treatment with mitomycin C and bortezomib was significantly more effective in inhibiting tumor growth compared with single treatment ($P < 0.01$). In Fig. 6C, H&E and CEA (used as a tumor marker) staining show that all the sections were in the tumor tissue. We also observed a decrease in Ki67 expression during treatment with mitomycin C and bortezomib, especially in the combinatorial treatment (Fig. 6C). In Figs. 6D and 6E, tumor tissue was stained for detection of both cleaved caspase 3 (green) and pimonidazole adducts (red), and analyzed (inset of Fig. 6D) and then histograms were drawn. We observed increased cleaved caspase 3 staining in the combinatorial treatment compared with single treatment ($P < 0.05$). Notably, we also observed that mitomycin C and the combinatorial treatment had more cleaved caspase 3 staining under hypoxia ($P < 0.05$). Fig. 6F shows a schematic diagram that explains how the combinatorial treatment with mitomycin C and bortezomib effectively induced apoptosis under hypoxia through Bak activation (oligomerization), Bcl-xL dissociation (Bcl-xL phosphorylation) and p53 translocation to the mitochondria.

Discussion

Malignant tumors contain hypoxic regions due to insufficient blood supply and can adapt and survive under hypoxic conditions with increased survival signaling and loss of apoptotic potential (33). Given the central role of hypoxia in tumor progression and resistance to therapy, it is worth exploiting validated treatments for targeting hypoxia for therapy of CPC. In this study, we observed that a combinatorial treatment with the bioreductive prodrug mitomycin C and the proteasome inhibitor bortezomib synergistically induced apoptosis in colorectal cancer cells and the peritoneal animal model under both normoxic and hypoxic conditions, and we also investigated the underlying mechanisms of mitomycin C- and bortezomib-induced apoptosis under hypoxia.

There are two main approaches for targeting hypoxia: bioreductive prodrugs and inhibitors of molecular targets upon which hypoxic cell survival depends. Prodrugs include five different chemical moieties (nitro groups, quinones, aromatic N-oxides, aliphatic N-oxides, and transition metals), which have the potential to be metabolized by enzymatic reduction under hypoxic conditions (7). The quinone mitomycin C is preferentially activated in hypoxic tumor cells (34). However, the detailed mechanisms of how mitomycin C

selectively induces the apoptotic death of hypoxic colorectal cancer cells have been poorly studied. In this study, we observed that p53 preferentially translocated to the mitochondria under hypoxia during treatment with mitomycin C (Fig. 5C).

The tumor suppressor gene p53 has multiple functions, including cell cycle regulation, DNA repair, and apoptosis. p53-associated apoptotic regulation can be achieved in a transcription-dependent or -independent manner. Death signals have been reported to be able to induce p53 translocation to the mitochondria via the transcription-independent apoptotic signal (35–38). p53 participates directly in the intrinsic apoptosis pathway by interacting with the multidomain members of the Bcl-2 family to induce mitochondrial outer membrane permeabilization, regardless of several common mutations (39–41). In the present studies, we observed that for mitomycin C, the combinatorial treatment, as well as hypoxic conditions, induced translocation of p53 protein to the mitochondria, while the application of bortezomib had a limited effect on p53 elevation and mitochondrial translocation. Recently, some novel molecules, such as Tid1(42), anionic phospholipids(36), dynamin-related protein 1(43), DJ-1(44), etc., have been reported to regulate the function of p53 translocation to the mitochondria. The possible involvement of these molecules in the mitochondrial translocation of p53 during treatment with mitomycin C and bortezomib, especially under hypoxia, needs to be elucidated in the near future.

It is obvious that mitomycin C alone is not enough to trigger sustained apoptosis, even with the dramatic translocation of p53 to the mitochondria upon hypoxia, which strongly indicates that a combination of other drugs is needed to induce conformational activation of pro-apoptotic Bak. We reported here that bortezomib enhanced the apoptotic effect of mitomycin C in several different colorectal cancer cells under both normoxic and hypoxic conditions. We propose that further liberation of Bak, specifically from the p53-activated Bak-Bcl-xL complex, is a prerequisite for inducing robust apoptosis.

We previously reported that Bcl-xL, a key antiapoptotic molecule, undergoes phosphorylation in several different treatments (30, 45, 46). We report here that activation of p38 and JNK are both specifically required for the combinatorial treatment with mitomycin C and bortezomib, which is in agreement with other observations (28, 47). The fact that a validated phospho-defective Bcl-xL mutant was resistant to the combinatorial treatment of oxaliplatin and bortezomib-induced apoptosis and retained the interaction between Bak and Bcl-xL, indicated that Bcl-xL phosphorylation at Ser 62 is a key regulatory mechanism for antagonizing antiapoptotic function in the combinatorial treatment. Thus, the mode of action of the synergistic effect of the DNA-damaging drug mitomycin C and proteasome inhibitor bortezomib is mediated via p53 mitochondrial translocation and phosphorylation of Bcl-xL which results in facilitating the disruption of the mitochondrial apoptosis effector Bak. Our results support a concept that coordinated cell-intrinsic death signals enhances in robust apoptosis.

Taken together, we presented here a novel combinatorial treatment with the chemotherapeutic agent mitomycin C and the proteasome inhibitor bortezomib, which induced synergistic apoptosis under both normoxic and hypoxic conditions through p53 translocation to the mitochondria and Bcl-xL phosphorylation, and further disruption of the

mitochondrial apoptosis effector Bak. Mitomycin C and bortezomib are both commonly used drugs that are approved by the US Food and Drug Administration and could be considered for CPC patients in clinics in the near future.

Acknowledgments

The authors thank Dr. Timothy C. Chambers (University of Arkansas for Medical Sciences, Little Rock, AR, USA) who provided pBcl-xL-WT and pBcl-xL-S62A.

Grant Support

This work was supported by the following grants: NCI grant R01CA140554 (Y.J.L.) and Basic Science Research Program of the National Research Foundation of Korea funded by the Ministry of Science, ICT and Future Planning: NRF-2013R1A2A2A01014170 (Y.T.K.). This project used the UPCI Core Facility and was supported in part by award P30CA047904.

Abbreviations used in this paper

Bak	Bcl-2 homologous antagonist/killer
Bax	Bcl-2–associated X protein
CEA	carcinoembryonic antigen
CI	combination index
DAPI	4′,6-diamidino-2-phenylindole
FBS	fetal bovine serum
FITC	fluorescein isothiocyanate
H&E	hematoxylin and eosin
HA	hemagglutinin
HIF	hypoxia-inducible factor
i.p	intraperitoneally
JNK	c-Jun NH2-terminal kinase
MAPK	mitogen-activated protein kinase
PARP	poly (ADP-ribose) polymerase
PC	peritoneal carcinomatosis
PBS	phosphate buffered saline
PI	propidium iodide
SDS-PAGE	sodium dodecyl sulfate polyacrylamide gel electrophoresis
S62	serine 62

References

1. Seidl C, Essler M. Radioimmunotherapy for peritoneal cancers. Immunotherapy. 2013; 5:395–405. [PubMed: 23557422]

2. Knorr C, Reingruber B, Meyer T, Hohenberger W, Stremmel C. Peritoneal carcinomatosis of colorectal cancer: incidence, prognosis, and treatment modalities. Int J Colorectal Dis. 2004; 19:181–7. [PubMed: 12955416]

3. Confuorto G, Giuliano ME, Grimaldi A, Viviano C. Peritoneal carcinomatosis from colorectal cancer: HIPEC? Surg Oncol. 2007; 16 (Suppl 1):S149–52. [PubMed: 18257149]

4. Yan TD, Morris DL. Cytoreductive surgery and perioperative intraperitoneal chemotherapy for isolated colorectal peritoneal carcinomatosis: experimental therapy or standard of care? Ann Surg. 2008; 248:829–35. [PubMed: 18948811]

5. Braicu EI, Luketina H, Richter R, Cacsire Castillo-Tong D, Lambrechts S, Mahner S, et al. HIF1alpha is an independent prognostic factor for overall survival in advanced primary epithelial ovarian cancer - a study of the OVCAD Consortium. Onco Targets Ther. 2014; 7:1563–9. [PubMed: 25246800]

6. Wilson WR, Hay MP. Targeting hypoxia in cancer therapy. Nat Rev Cancer. 2011; 11:393–410. [PubMed: 21606941]

7. Rooseboom M, Commandeur JN, Vermeulen NP. Enzyme-catalyzed activation of anticancer prodrugs. Pharmacol Rev. 2004; 56:53–102. [PubMed: 15001663]

8. Lou JJ, Chua YL, Chew EH, Gao J, Bushell M, Hagen T. Inhibition of hypoxia-inducible factor-1alpha (HIF-1alpha) protein synthesis by DNA damage inducing agents. PLoS One. 2010; 5:e10522. [PubMed: 20479887]

9. Van der Speeten K, Stuart OA, Chang D, Mahteme H, Sugarbaker PH. Changes induced by surgical and clinical factors in the pharmacology of intraperitoneal mitomycin C in 145 patients with peritoneal carcinomatosis. Cancer Chemother Pharmacol. 2011; 68:147–56. [PubMed: 20857115]

10. Thakur JS, Chauhan CG, Diwana VK, Chauhan DC, Thakur A. Extravasational side effects of cytotoxic drugs: A preventable catastrophe. Indian J Plast Surg. 2008; 41:145–50. [PubMed: 19753254]

11. Fujimoto S, Takahashi M, Mutou T, Kobayashi K, Toyosawa T, Kondoh K, et al. Survival time and prevention of side effects of intraperitoneal hyperthermic perfusion with mitomycin C combined with surgery for patients with advanced gastric cancer. Cancer Treat Res. 1996; 81:169–76. [PubMed: 8834583]

12. Cohen MS, Al-Kasspooles MF, Williamson SK, Henry D, Broward M, Roby KF. Combination intraperitoneal chemotherapy is superior to mitomycin C or oxaliplatin for colorectal carcinomatosis in vivo. Ann Surg Oncol. 2010; 17:296–303. [PubMed: 19707832]

13. Kornek GV, Schuell B, Laengle F, Gruenberger T, Penz M, Karall K, et al. Mitomycin C in combination with capecitabine or biweekly high-dose gemcitabine in patients with advanced biliary tract cancer: a randomised phase II trial. Ann Oncol. 2004; 15:478–83. [PubMed: 14998852]

14. Saif MW, Kaley K, Brennan M, Garcon MC, Rodriguez G. Mitomycin-C and capecitabine (MIXE) as salvage treatment in patients with refractory metastatic colorectal cancer: a retrospective study. Anticancer Res. 2013; 33:2743–6. [PubMed: 23749935]

15. Borczuk AC, Cappellini GC, Kim HK, Hesdorffer M, Taub RN, Powell CA. Molecular profiling of malignant peritoneal mesothelioma identifies the ubiquitin-proteasome pathway as a therapeutic target in poor prognosis tumors. Oncogene. 2007; 26:610–7. [PubMed: 16862182]

16. Nikiforov MA, Riblett M, Tang WH, Gratchouck V, Zhuang D, Fernandez Y, et al. Tumor cell-selective regulation of NOXA by c-MYC in response to proteasome inhibition. Proceedings of the National Academy of Sciences of the United States of America. 2007; 104:19488–93. [PubMed: 18042711]

17. Mangiacavalli S, Pochintesta L, Pascutto C, Cocito F, Pompa A, Cazzola M, et al. Good clinical activity and favorable toxicity profile of once weekly bortezomib, fotemustine, and dexamethasone (B-MuD) for the treatment of relapsed multiple myeloma. Am J Hematol. 2013; 88:102–6. [PubMed: 23224960]

18. Wu KL, van Wieringen W, Vellenga E, Zweegman S, Lokhorst HM, Sonneveld P. Analysis of the efficacy and toxicity of bortezomib for treatment of relapsed or refractory multiple myeloma in community practice. Haematologica. 2005; 90:996–7. [PubMed: 15996946]

19. Aghajanian C, Blessing JA, Darcy KM, Reid G, DeGeest K, Rubin SC, et al. A phase II evaluation of bortezomib in the treatment of recurrent platinum-sensitive ovarian or primary peritoneal cancer: a Gynecologic Oncology Group study. Gynecologic oncology. 2009; 115:215–20. [PubMed: 19712963]
20. Parma G, Mancari R, Del Conte G, Scambia G, Gadducci A, Hess D, et al. An open-label phase 2 study of twice-weekly bortezomib and intermittent pegylated liposomal doxorubicin in patients with ovarian cancer failing platinum-containing regimens. International journal of gynecological cancer : official journal of the International Gynecological Cancer Society. 2012; 22:792–800. [PubMed: 22635029]
21. Marxsen JH, Stengel P, Doege K, Heikkinen P, Jokilehto T, Wagner T, et al. Hypoxia-inducible factor-1 (HIF-1) promotes its degradation by induction of HIF-alpha-prolyl-4-hydroxylases. Biochem J. 2004; 381:761–7. [PubMed: 15104534]
22. Bilton RL, Booker GW. The subtle side to hypoxia inducible factor (HIFalpha) regulation. Eur J Biochem. 2003; 270:791–8. [PubMed: 12603312]
23. Zhou Z, Liu F, Zhang ZS, Shu F, Zheng Y, Fu L, et al. Human rhomboid family-1 suppresses oxygen-independent degradation of hypoxia-inducible factor-1alpha in breast cancer. Cancer research. 2014; 74:2719–30. [PubMed: 24648344]
24. Zhu Y, Regunath K, Jacq X, Prives C. Cisplatin causes cell death via TAB1 regulation of p53/MDM2/MDMX circuitry. Genes Dev. 2013; 27:1739–51. [PubMed: 23934659]
25. Mancini F, Moretti F. Mitochondrial MDM4 (MDMX): an unpredicted role in the p53-mediated intrinsic apoptotic pathway. Cell cycle. 2009; 8:3854–9. [PubMed: 19887911]
26. Mancini F, Gentiletti F, D'Angelo M, Giglio S, Nanni S, D'Angelo C, et al. MDM4 (MDMX) overexpression enhances stabilization of stress-induced p53 and promotes apoptosis. J Biol Chem. 2004; 279:8169–80. [PubMed: 14660608]
27. Mancini F, Di Conza G, Pellegrino M, Rinaldo C, Prodosmo A, Giglio S, et al. MDM4 (MDMX) localizes at the mitochondria and facilitates the p53-mediated intrinsic-apoptotic pathway. Embo J. 2009; 28:1926–39. [PubMed: 19521340]
28. Wang J, Beauchemin M, Bertrand R. Phospho-Bcl-xL(Ser62) influences spindle assembly and chromosome segregation during mitosis. Cell cycle. 2014; 13:1313–26. [PubMed: 24621501]
29. Basu A, Haldar S. Identification of a novel Bcl-xL phosphorylation site regulating the sensitivity of taxol- or 2-methoxyestradiol-induced apoptosis. FEBS letters. 2003; 538:41–7. [PubMed: 12633850]
30. Song X, Kim SY, Lee YJ. The role of Bcl-xL in synergistic induction of apoptosis by mapatumumab and oxaliplatin in combination with hyperthermia on human colon cancer. Molecular cancer research : MCR. 2012; 10:1567–79. [PubMed: 23051936]
31. Wei MC, Zong WX, Cheng EH, Lindsten T, Panoutsakopoulou V, Ross AJ, et al. Proapoptotic BAX and BAK: a requisite gateway to mitochondrial dysfunction and death. Science. 2001; 292:727–30. [PubMed: 11326099]
32. Carethers JM, Pham TT. Mutations of transforming growth factor beta 1 type II receptor, BAX, and insulin-like growth factor II receptor genes in microsatellite unstable cell lines. In Vivo. 2000; 14:13–20. [PubMed: 10757056]
33. Brahimi-Horn MC, Chiche J, Pouyssegur J. Hypoxia and cancer. Journal of molecular medicine. 2007; 85:1301–7. [PubMed: 18026916]
34. Kennedy KA, Rockwell S, Sartorelli AC. Preferential activation of mitomycin C to cytotoxic metabolites by hypoxic tumor cells. Cancer research. 1980; 40:2356–60. [PubMed: 7388797]
35. Marchenko ND, Zaika A, Moll UM. Death signal-induced localization of p53 protein to mitochondria. A potential role in apoptotic signaling. J Biol Chem. 2000; 275:16202–12. [PubMed: 10821866]
36. Li CH, Cheng YW, Liao PL, Kang JJ. Translocation of p53 to mitochondria is regulated by its lipid binding property to anionic phospholipids and it participates in cell death control. Neoplasia. 2010; 12:150–60. [PubMed: 20126473]
37. Sansome C, Zaika A, Marchenko ND, Moll UM. Hypoxia death stimulus induces translocation of p53 protein to mitochondria. Detection by immunofluorescence on whole cells. FEBS letters. 2001; 488:110–5. [PubMed: 11163756]

38. Wang Y, Pakunlu RI, Tsao W, Pozharov V, Minko T. Bimodal effect of hypoxia in cancer: role of hypoxia inducible factor in apoptosis. Mol Pharm. 2004; 1:156–65. [PubMed: 15832512]
39. Vaseva AV, Moll UM. The mitochondrial p53 pathway. Biochim Biophys Acta. 2009; 1787:414–20. [PubMed: 19007744]
40. Charlot JF, Pretet JL, Haughey C, Mougin C. Mitochondrial translocation of p53 and mitochondrial membrane potential (Delta Psi m) dissipation are early events in staurosporine-induced apoptosis of wild type and mutated p53 epithelial cells. Apoptosis : an international journal on programmed cell death. 2004; 9:333–43. [PubMed: 15258465]
41. Kim H, Moon JY, Ahn KS, Cho SK. Quercetin induces mitochondrial mediated apoptosis and protective autophagy in human glioblastoma U373MG cells. Oxid Med Cell Longev. 2013; 2013:596496. [PubMed: 24379902]
42. Ahn BY, Trinh DL, Zajchowski LD, Lee B, Elwi AN, Kim SW. Tid1 is a new regulator of p53 mitochondrial translocation and apoptosis in cancer. Oncogene. 2010; 29:1155–66. [PubMed: 19935715]
43. Guo X, Sesaki H, Qi X. Drp1 stabilizes p53 on the mitochondria to trigger necrosis under oxidative stress conditions in vitro and in vivo. Biochem J. 2014; 461:137–46. [PubMed: 24758576]
44. Ottolini D, Cali T, Negro A, Brini M. The Parkinson disease-related protein DJ-1 counteracts mitochondrial impairment induced by the tumour suppressor protein p53 by enhancing endoplasmic reticulum-mitochondria tethering. Hum Mol Genet. 2013; 22:2152–68. [PubMed: 23418303]
45. Song X, Kim SY, Lee YJ. Evidence for two modes of synergistic induction of apoptosis by mapatumumab and oxaliplatin in combination with hyperthermia in human colon cancer cells. PLoS One. 2013; 8:e73654. [PubMed: 24013390]
46. Kim SY, Song X, Zhang L, Bartlett DL, Lee YJ. Role of Bcl-xL/Beclin-1 in interplay between apoptosis and autophagy in oxaliplatin and bortezomib-induced cell death. Biochemical pharmacology. 2014; 88:178–88. [PubMed: 24486574]
47. Bah N, Maillet L, Ryan J, Dubreil S, Gautier F, Letai A, et al. Bcl-xL controls a switch between cell death modes during mitotic arrest. Cell Death Dis. 2014; 5:e1291. [PubMed: 24922075]

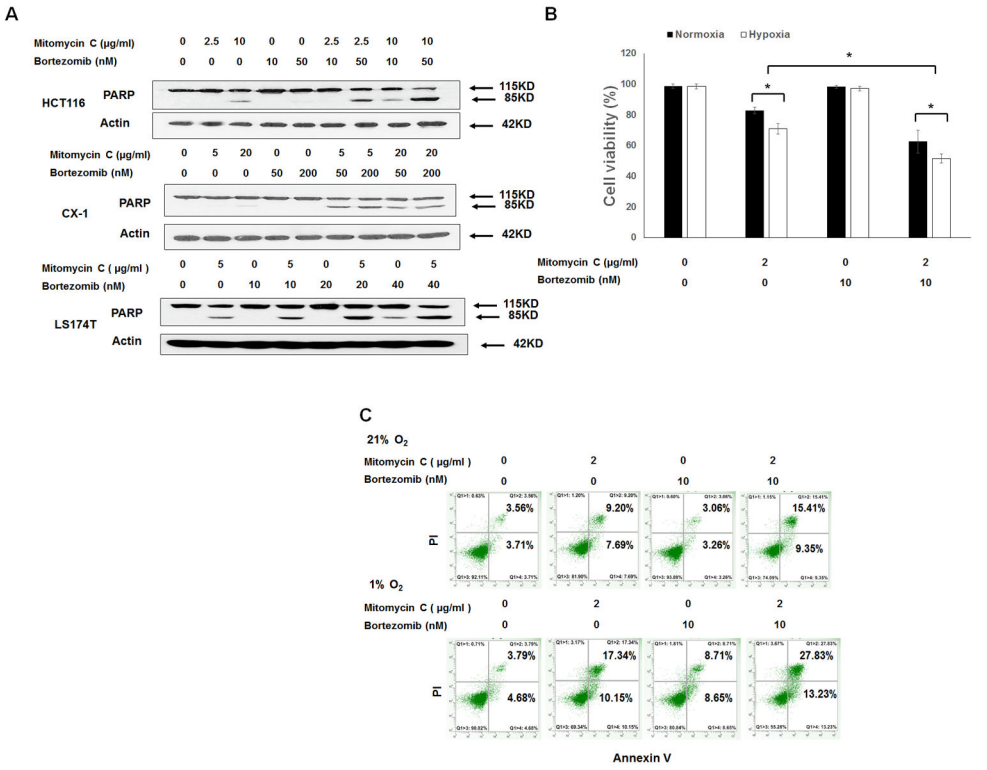

Figure 1. The combination of mitomycin C and bortezomib induced synergistic apoptosis in colorectal cancer cell lines

(**A**) HCT116, CX-1, and LS174T cells were treated with mitomycin C (5–20 μg/ml) and/or bortezomib (10–200 nM) for 24 h. After treatment, PARP was detected with immunoblotting. Actin was used to confirm equal amounts of proteins loaded in each lane. (**B**) LS174T cells were treated with mitomycin C (2 μg/ml) and/or bortezomib (10 nM) under normoxic (21% O_2) and hypoxic (1% O_2) conditions for 24 h. Cell viability was analyzed via MTS assay. Error bars represent S.D. from triplicate experiments. Asterisks ** represents a statistically significant difference compared with the control group ($P < 0.01$). **(C)** After treatment, cells were stained with fluorescein isothiocyanate (FITC)-annexin V and propidium iodide (PI). Apoptosis was detected with flow cytometric assay.

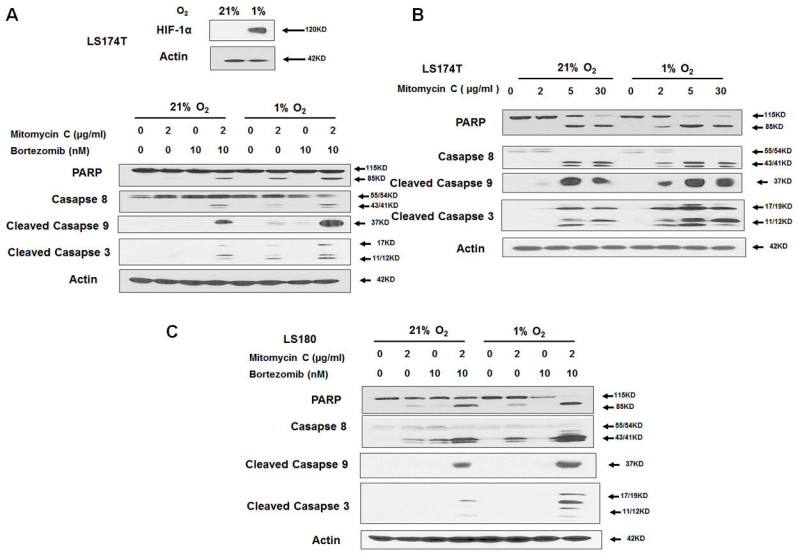

Figure 2. The combination of mitomycin C and bortezomib induced significant activation of caspases under hypoxia

(A) LS174T cells were exposed to normoxia and hypoxia for 24 h and the intracellular level of hypoxia-inducible factor-1α (HIF-1α) was detected with immunoblotting (inset). LS174T cells were treated with mitomycin C (2 μg/ml) and/or bortezomib (10 nM) under normoxia and hypoxia for 24 h and caspase 8, cleaved caspase 9, and cleaved caspase 3 were detected with immunoblotting (main). (**B**) LS174T cells were treated with mitomycin C (2, 5, 30 μg/ml) under normoxia and hypoxia for 24 h and caspase 8, cleaved caspase 9, and cleaved caspase 3 were detected with immunoblotting. **(C)** LS180 cells were treated with mitomycin C (2 μg/ml) and bortezomib (10 nM) under normoxia and hypoxia for 24 h and caspase 8, cleaved caspase 9, and cleaved caspase 3 were detected with immunoblotting. Actin was used to confirm equal amounts of proteins loaded in each lane.

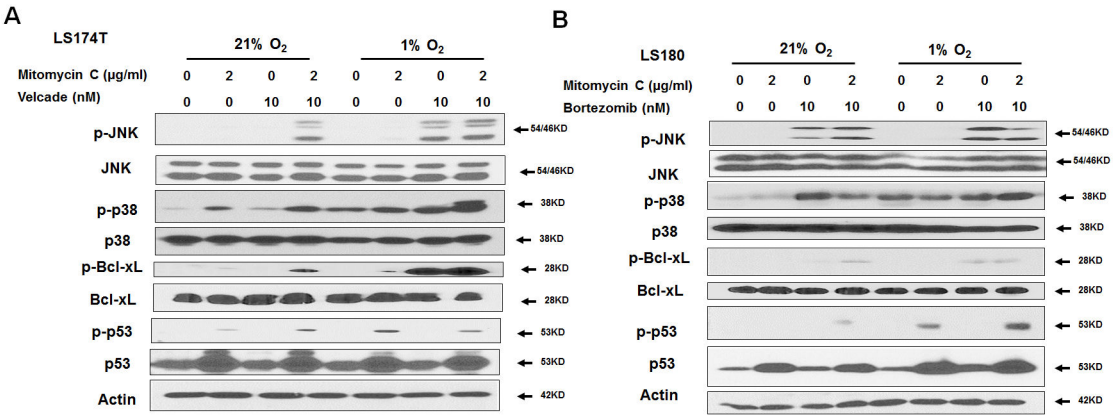

Figure 3. The combination of mitomycin C and bortezomib induced Bcl-xL phosphorylation and p53 elevation under normoxia and hypoxia

LS174T (**A**) and LS180 (**B**) cells were treated with mitomycin C (2 μg/ml) and/or bortezomib (10 nM) under normoxia and hypoxia for 24 h and p-JNK/JNK, p-p38/p38, p-Bcl-xL/Bcl-xL, and p-p53(Ser46)/p53 were detected with immunoblotting. Actin was used to confirm equal amounts of proteins loaded in each lane.

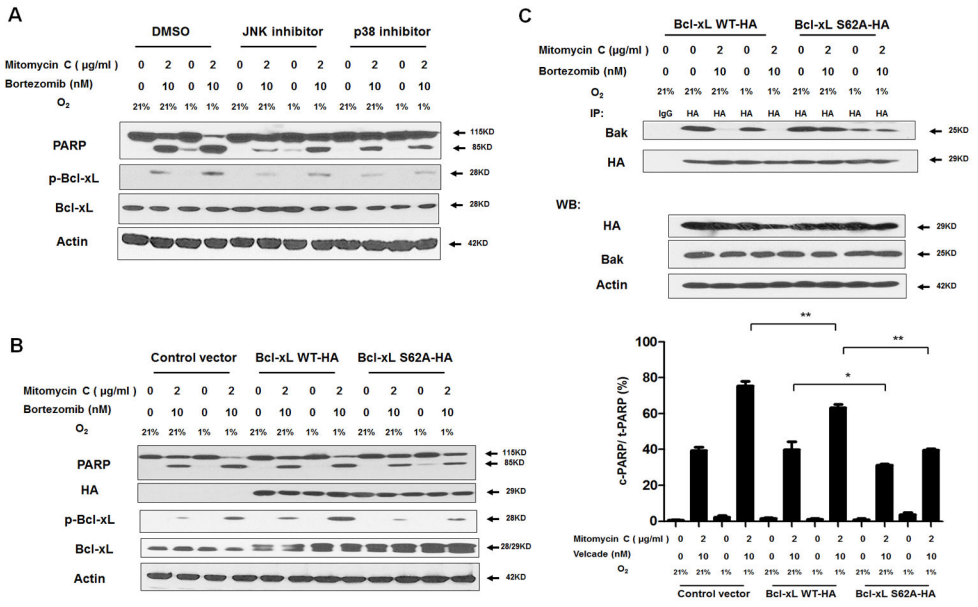

Figure 4. Role of Bcl-xL phosphorylation in the combinatorial treatment with mitomycin C and bortezomib under normoxia and hypoxia

(**A**) LS174T cells were pretreated with 20 μM SP600125 or 10 μM SB203580 for 30 min followed by mitomycin C (2 μg/ml) and/or bortezomib (10 nM) under normoxia and hypoxia for 24 h. PARP cleavage and p-Bcl-xL/Bcl-xL were detected with immunoblotting. **(B) Left panel:** LS174T cells were transiently transfected with a sham plasmid, Bcl-xL WT-HA and Bcl-xL S62A-HA; 48 h later, cells were treated with mitomycin C (2 μg/ml) and bortezomib (10 nM) under normoxia and hypoxia for 24 h. PARP, HA, and p-Bcl-xL/Bcl-xL were detected with immunoblotting. Actin was shown as an internal control. **Right panel:** Densitometry analysis of c-PARP/PARP of the band in the left panel was performed. Error bars represent SD from triplicate experiments. **(C)** After treatment, cell lysates were immunoprecipitated with anti-HA antibody or IgG and then immunoblotted with anti-Bak antibody. The presence of HA and Bak in the lysates was examined.

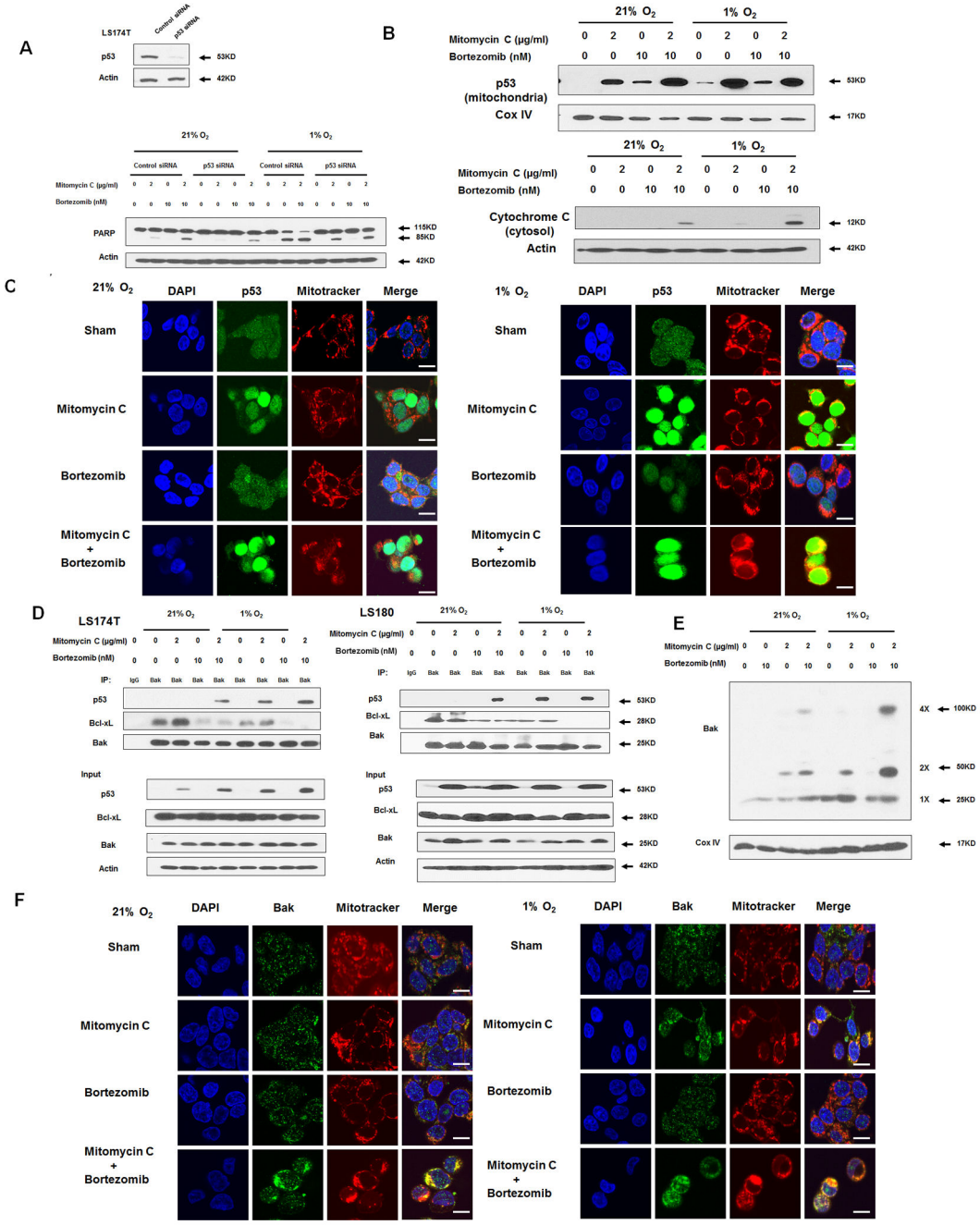

Figure 5. Role of p53 in the combinatorial treatment with mitomycin C and bortezomib under normoxia and hypoxia

(A) LS174T cells were transfected with control siRNA or p53 siRNA for 48 h and the level of p53 was detected by immunoblotting (inset). After 48 h transfection, cells were treated with mitomycin C (2 μg/ml) and/or bortezomib (10 nM) under normoxia and hypoxia for 24 h (main). PARP was detected with immunoblotting. The levels of p53 were detected by immunoblotting 72 h after transfection. Actin was used as a loading control. **(B)** LS174T cells were treated with mitomycin C (2 μg/ml) and/or bortezomib (10 nM) under normoxia and hypoxia for 24 h. After treatment, cytosolic and mitochondrial fractions were isolated

and p53 was detected in mitochondrial fractions with immunoblotting. The results of the COX IV analysis are shown as an internal mitochondrial control. Actin was used as an internal cytosol control. **(C)** After treatment, mitochondria were stained with MitoTracker. p53 was stained with anti-p53 antibody. Localization of p53 was examined by confocal microscope. Scale bar 15 μm. **(D)** LS174T cells and LS180 cells were treated with mitomycin C (2 μg/ml) and/or bortezomib (10 nM) under normoxia and hypoxia for 24 h. After treatment, cell lysates were immunoprecipitated with anti-Bak antibody or IgG and immunoblotted with anti-p53 and anti-Bcl-xL antibody. The presence of Bak, p53 and Bcl-xL in the lysates was examined. **(E)** LS174T cells were treated with mitomycin C (5 μg/ml) and/or bortezomib (10 nM) in normoxia and hypoxia for 24 h. After treatment, mitochondria were isolated, cross-linked with 1 mM dithiobis (succinimidyl propionate) and subjected to immunoblotting with anti-Bak antibody. Bak monomer (1X) and multimers (2X and 4X) are indicated. COX IV was used as a mitochondrial marker. Scale bar 15 μm. **(F)** After treatment, mitochondria were stained with MitoTracker. Bak was stained with anti-Bak antibody. Localization of Bak was examined under confocal microscope.

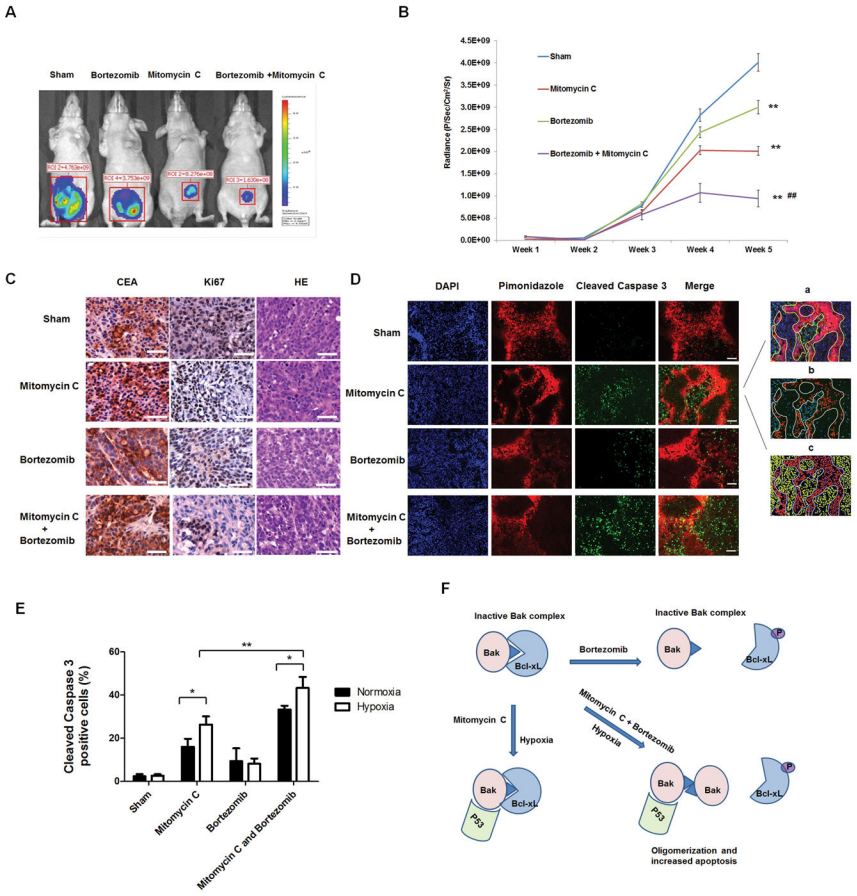

Figure 6. Effect of mitomycin C and bortezomib on the growth of LS174T intraperitoneal tumors

(A) Nude mice were intraperitoneally (i.p.) inoculated with 5×10^5 LS174T-luc cells/mouse on day 0. Four days after tumor inoculation, all the tumor-bearing mice were treated with either phosphate buffered saline (PBS) alone (sham) or bortezomib alone at a dose of (0.25 mg/kg body weight) or mitomycin C (1.5 mg/kg body weight) alone or the combination of mitomycin C and bortezomib every other day from day 4 to day 28. Mice were imaged using the IVIS Imaging System Series 200. ** represents a statistically significant difference ($P<0.01$) compared with the control group. ## represents a statistically significant difference ($P<0.01$) compared with the single treatment group **(B)** Line graph illustrating the luciferase activity (photons/second) in LS174T tumor-bearing mice treated with PBS alone, bortezomib alone, mitomycin C alone, or the combination from week 1 to week 5. **(C)** Tumor tissues were harvested at week 5 and subjected to H&E staining and immunohistochemistry staining with anti-CEA and ki67 primary antibodies. Representative images are shown (magnification, X400). Scale bar 50 μm. **(D)** Animals were sacrificed 1 h after pimonidazole injection (i.p.). Tissue was stained for cleaved caspase 3 (green) and pimonidazole adducts (red). Cell nuclei were stained with DAPI. Representative images are shown (magnification, X200). Scale bar 100 μm. Quantification was performed with Photoshop software: (a) Hypoxic region was determined by the yellow shape. (b) Cleaved caspase 3-positive cells were quantifed. (c) Cell nuclei were quantified. **(E)** Cleaved caspase 3-positive cells in normoxic and hypoxic areas were quantified. *$P<0.05$; ** $P<0.01$. **(G)** A

schematic diagram of the mechanism of the combinatorial treatment with mitomycin C and bortezomib-induced apoptosis under hypoxia.

Table 1

Combination Index (CI) for the combination of mitomycin C and bortezomib under hypoxia (1% O_2) was calculated using the CompuSyn software for LS174T and LS180 cancer cells.

Combination therapy		Combination index	
Mitomycin C (μg/ml)	**Bortezomib (nM)**	**LS174T**	**LS180**
2	10	0.24 ***	0.25***
4	20	0.41**	0.33**
10	30	0.47**	0.41**

* slight synergy;

** moderate synergy;

*** strong synergy.